

## Anticorrosive Performance of Vinyl Butyral-co-vinyl alcohol-co-vinyl Acetate Based Copolymer Adsorbed on Steel Surfaces. Electrochemical and AFM Studies

Claudia Merișanu<sup>1,2</sup>, Adriana Samide<sup>1,\*</sup>, Gabriela Eugenia Iacobescu<sup>3,\*</sup>, Bogdan Tutunaru<sup>1</sup>, Cristian Tigae<sup>1</sup>, Alexandru Popescu<sup>2</sup>

<sup>1</sup> University of Craiova, Faculty of Sciences, Department of Chemistry, 107i Calea Bucuresti, Craiova, Romania

<sup>2</sup> University of Craiova, Faculty of Sciences, Doctoral School of Sciences, A.I. Cuza no.13, Craiova, Romania

<sup>3</sup> University of Craiova, Faculty of Sciences, Department of Physics, A.I. Cuza no.13, Craiova, Romania

\*E-mail: [samide\\_adriana@yahoo.com](mailto:samide_adriana@yahoo.com); [gabrielaiacobescu@yahoo.com](mailto:gabrielaiacobescu@yahoo.com)

Received: 6 May 2020 / Accepted: 14 July 2020 / Published: 31 August 2020

---

The copolymer film anticorrosive performance based on *poly(vinyl butyral-co-vinyl alcohol-co-vinyl acetate)*, called in this study as PVBA, deposited by the dipping method on the carbon steel and 304L stainless steel surfaces from methanolic solution was studied by open circuit potential (OCP) measurements, potentiodynamic polarization and electrochemical impedance spectroscopy (EIS). The morphological characteristics of the uncovered and covered surfaces with copolymer film, before and after corrosion were identified by atomic force microscopy (AFM). The average protection performance (P%) of PVBA adsorbed on metallic surfaces corroded in 0.9% NaCl solution reached the value of  $64 \pm 2\%$  for carbon steel and  $72 \pm 2\%$ , respectively, for 304L stainless steel. AFM 3D images, before corrosion, display coherently organized coatings adsorbed on the surfaces of steels, with a network characteristic, more obviously in the case of 304L stainless steel than that of carbon steel. After corrosion, AFM shows that the surface upper-layers preserve their features, suggesting that the coating remains anchored to the metal surface for a long time, but the polymer swelling in NaCl solution causes the relative detachment of the film from the substrate, with the formation of some free areas on which the oxidation processes can be accelerated, leading to PVBA anticorrosive performance disturbance.

---

**Keywords:** PVBA copolymer; Carbon steel and 304L Stainless steel; Anticorrosive coating; Electrochemical measurements; Atomic force microscopy (AFM)

### 1. INTRODUCTION

The different steel types are alloys susceptible to corrosion, the majority element in their composition being the iron, that is the most vulnerable to oxidation processes at the surface contact with

aggressive media. Thus, in order to restrict the damage of the metallic surfaces and at the same time to increase the corrosion resistance, anticorrosive coatings can be applied by the adsorption of some polymers/copolymers leading to the occurrence of thin films that attach from the metallic surfaces through the chemical/physical bonds. Polymers and copolymers are an efficient choice for the functionalization of metal surfaces because they have numerous active centers distributed along their macromolecular chains, through which they can adsorb on the substrate forming coherently organized films with anticorrosive properties.

In this regard, polyvinyl alcohol [1] and polyvinyl acetate [2-4] were investigated as corrosion inhibitors for carbon/mild steel [1-4] and stainless steel [5-8] in hydrochloric acid solution [1-3, 5], sulfuric acid [4] or in saline environments [6-8], using mass loss method associated with electrochemical measurements. Natural polymer like chitosan was tested as corrosion inhibitor for mild steel in 0.1 mol L<sup>-1</sup> HCl solution by electrochemical measurements coupled with scanning electron microscopy (SEM), finding an inhibition efficiency of 96%, at 60 °C [9].

Microfibers based on vinyl ester polymer [10], silane [11] and aniline, formaldehyde and piperazine based polymer [12] were also used as anticorrosive coatings for carbon/mild/N80 [10-12] steel in chloride ion solution reaching a good surface protection performance. Conducting copolymers provide a wide variety of functional copolymers with application in anticorrosive coatings [13-17].

Also, efficient anticorrosive coatings for different steel types can be prepared by adsorption of copolymers, thus modeling thin films that change the surface architecture, improving its characteristics [18-21].

Many polymers are ecological, biodegradable, biocompatible compounds, without toxic and carcinogenic effects, being applied in numerous industrial and medical fields. Moreover, macromolecular networks based on polyvinyl butyral have special characteristics such as "shape memory" [22-24], thus having the ability to self-regenerate, recovering their initial shapes after the application of an electrical, magnetic or thermal stimulus, leading to the preservation of the metallic surface properties covered with polymer film, after exposure in aggressive environments for a long time. The application of polymers as corrosion inhibitors in aqueous media is sometimes limited, these being water insoluble compounds, but soluble in various organic solvents. For this reason, their testing as anticorrosive agents in aqueous media requires the use of appropriate film deposition methods, which remove the inconveniences caused by insolubility.

Thus, the assembly of protective layers based on polymers can be performed by several methods, as follows: (1) electro-polymerization on metallic electrodes using cyclic voltammetry [25]; (2) preparation an aqueous dispersion medium by emulsion polymerization, which allows the investigation of the inhibitory and adsorption properties of the respective polymer [2]; (3) functionalization of metallic surfaces by polymer adsorption from a specific organic solvent [24].

In this study, it was determined the protection performance of copolymer based on poly(vinyl butyral-co-vinyl alcohol-co-vinyl acetate), named as PVBA, adsorbed on the carbon steel and 304L stainless steel surfaces from methanol solution using the simple dipping method of metal samples, a well determined time. In this regard, the corrosion resistance of the uncoated (CS, SS) and coated samples (CS-PVBA, SS-PVBA) corresponding to carbon steel (CS, CS-PVBA) and 304L stainless steel (SS, SS-

PVBA), in 0.9% NaCl solution was comparatively evaluated by electrochemical measurements and atomic force microscopy (AFM).

This investigation represents a continuation of our previous study, where the anticorrosive performance of the copolymer film adsorbed on copper surface was reported [24].

## 2. MATERIALS AND METHODS

### 2.1. Materials

Two types of steel (carbon steel and 304L stainless steel) were used in our experiments to investigate the anticorrosion performance of an adsorbed copolymer coating on their surfaces subjected to successive electrochemical measurements such as potential variation at open circuit, electrochemical impedance spectroscopy (EIS) and potentiodynamic polarization. The plates with the area of 2.0 cm<sup>2</sup> were obtained from carbon steel foils, its composition (wt%) consisting of: 0.1-0.25% C; 0.035% Si, 0.4% Mn, 0.3% Cr, 0.3% Ni and Fe in balance, as well as from the sheets of 304L stainless steel (FeNi18Cr10) purchased from Sigma Aldrich.

The copolymer based on polyvinyl butyral/polyvinyl alcohol/polyvinyl acetate known as poly(vinyl butyral-co-vinyl alcohol-co-vinyl acetate) and further used with the acronym PVBA with the average molecular mass between 90000 and 120000 (acetate/hydroxyl/vinyl butyral, wt%: 1/11/88), as well as methyl alcohol, sodium chloride were obtained from Sigma Aldrich.

### 2.2. PVBA coating preparation

Untreated control samples of both steels were mechanically processed as in our previous study, when PVBA was used as an anticorrosive coating for copper [24], these being sanded, ultrasonically cleaned, degreased with acetone and dried in warm air. For PVBA thin film deposition a simple dipping method [24] was used based on immersion of specimens of steels in a methanolic solution containing 6.0% PVBA, at room temperature. After 24 hours, the samples were removed from the methanolic bath, dried at room temperature (24 h) and in warm air (2 h).

Carbon steel samples will be referred to as CS for the untreated sample and CS-PVBA for the one modified with copolymer coating, while the 304L stainless steel untreated sample will be further named as SS, and PVBA modified stainless steel as SS-PVBA.

All four classes mentioned above will be subjected to corrosion in 0.9% NaCl solution, and the results regarding the copolymer film anticorrosive performance will be comparatively discussed for each steel.

### 2.3. Corrosion tests

The corrosion behavior of both steels CS and SS untreated and PVBA treated samples was tested using electrochemical measurements such as: the open circuit potential (OCP) variation over time,

electrochemical impedance spectroscopy (EIS) and potentiodynamic polarization. The surface morphology changes were designed on the atomic force microscopy (AFM) acquired slides.

### 2.3.1. Electrochemical measurements

Electrochemical impedance spectroscopy (EIS) was performed in 0.9% NaCl solution, at corresponding OCP (electrode prepolarization time of 4 minutes) on uncoated (CS and SS) samples and PVBA coated surfaces (CS-PVBA and SS-PVBA), in the frequency range of  $10^5$  Hz and  $10^{-1}$  Hz, with a sinusoidal perturbation, AC signal of 10 mV.

After EIS, the potentiodynamic polarization was performed in 0.9% NaCl solution, at room temperature, on carbon steel electrodes, in the potential range between -1000 mV and 100 mV, and between -1000 mV and 1000 mV on 304L stainless steel, respectively, with a potential scan rate of  $1.0 \text{ mV s}^{-1}$ . The semilogarithmic polarization curves as well the linear diagrams were recorded. The corrosion current density ( $i_{\text{corr}}$ ) for uncoated and PVBA coated samples, of both steels, was computed at the intersection of Tafel lines extrapolated to corrosion potential ( $E_{\text{corr}}$ ). Also, the polarization resistance ( $R_p$ ) was calculated from the linear diagram drawn, in the potential range close to corrosion potential ( $\pm 20$  mV). The standard electrochemical cell of 100 mL volume, with three electrodes was coupled to an electrochemical system VoltaLab type with VoltaMaster 4 software. The untreated and PVBA treated samples of both steel types were sequentially used as working electrodes having a platinum plate as counter-electrode, and Ag/AgCl reference electrode. Also, the details about experimental methods and equipment were reported in our previous studies [24-30].

### 2.4. Atomic Force Microscopy (AFM)

The images 3D acquired by Atomic Force Microscopy (AFM) for CS, CS-PVBA, SS and SS-PVBA before and after corrosion were used to examine the surface morphological changes due to the copolymer coatings and to explain its action mechanism. As in our previous studies [24, 26-28], the AFM slides were obtained through non-contact mode atomic force microscopy (NC-AFM, Park Systems, Suwon, Korea, PARK XE-100 SPM system), with a cantilever nominal length of 125  $\mu\text{m}$ , a nominal force constant of  $40 \text{ N m}^{-1}$ , and oscillation frequencies in the frequency range of 275–373 kHz.

## 3. RESULTS AND DISCUSSION

### 3.1. Open circuit measurements

The open-circuit behavior of uncoated samples (CS and SS) and those covered with PVBA (CS-PVBA and SS-PVBA) tested in 0.9% NaCl solution is shown in Figure 1. It can observe that the CS-PVBA potential (Fig. 1a) has a slightly tendency to stabilize at a value relatively close to that of the CS. On the contrary, the potential of stainless steel coated with polymer (SS-PVBA in Fig. 1b) reaches a constant value, after 50 sec. Thus, a plateau was formed at potential greater than that of the SS, which

has a slightly increasing trend in this time range. Those mentioned above show that the metal surfaces modified with PVBA are more stable in NaCl solution than those of the uncoated samples. The presence of polymeric film leads to the open circuit potential displacement towards higher values indicating that PVBA coating confers to metallic surface uniformity and stability providing a better protection for stainless steel than the one for carbon steel.

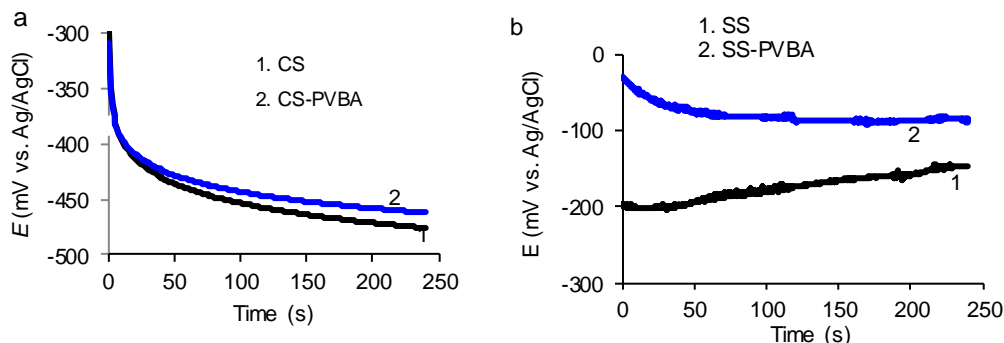


**Figure 1.** Open circuit potential variation of uncoated and coated steels in 0.9% NaCl solution: a – carbon steel; b – 304L stainless steel

### 3.2. Electrochemical impedance spectroscopy (EIS)

The Nyquist and Bode diagrams were recorded in sodium chloride solution, in the frequency range from  $10^5$  Hz to  $10^{-1}$  Hz, for uncoated and PVBA coated steels, their plots being displayed in Figures 2 and 3. Some similarities can be observed between the Nyquist diagrams (Fig. 2) of the two steels, namely: (1) in the presence of the polymeric film, capacitive loops with larger diameters than those obtained for the uncoated samples were registered; (2) in both cases, the extension of the capacitive loops implies a higher charge transfer resistance ( $R_{ct}$ ) of the PVBA coated steels than of the uncoated ones [24-26, 29, 30]. In the case of SS-PVBA, a large diameter loop was obtained (Fig. 2b) as opposed to the one with the closed semicircular shape registered for CS-PVBA (Fig. 2a), indicating a significant increase of the charge transfer resistance and consequently, a protection enhancement due to PVBA layer anchored on the 304L stainless steel surface compared to the PVBA film efficiency adsorbed on carbon steel surface.

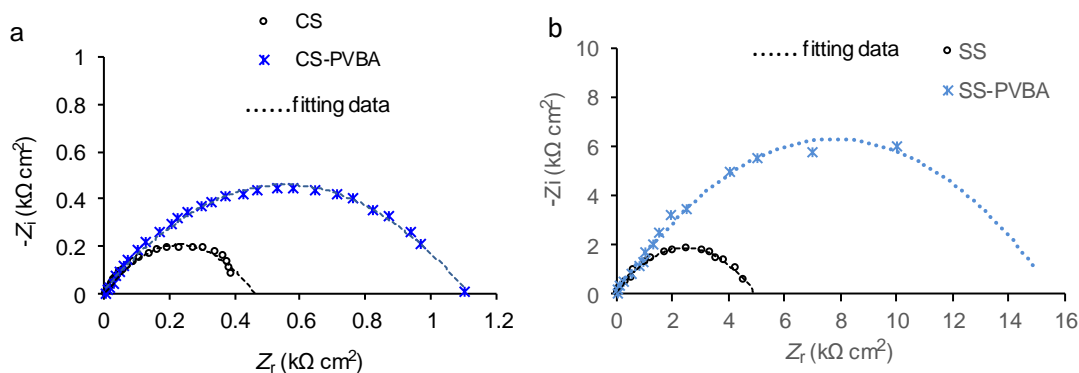


**Figure 2.** Nyquist diagrams recorded for uncovered and covered steels in 0.9% NaCl solution: a – carbon steel; b – 304L stainless steel

On the other hand, classical impedance responses were recorded, for the uncoated and coated samples with PVBA (Figs. 3a and 3b). For both coated samples, CS-PVBA and SS-PVBA, the impedance responses at low frequency ( $\log Z = -1$ ) reached upper levels compared to those of CS and SS, implying the attainment of higher impedance values conferred by the polymer adsorbed on the metallic surface, these being in good agreement with  $R_{ct}$  values (Table 1).

Phase Bode diagram of the carbon steel (Fig. 3c) shows a well-defined phase angle for the two samples, ranging from -59.9 degrees for CS to -63.1 degrees for CS-PVBA located at higher frequency *versus* uncoated steel, indicating the change in surface layer composition by the adsorption of PVBA macromolecules on the metallic surface.

On the contrary, in the case of stainless steel, the Bode diagram (Fig. 3d) shows an undefined wide maximum located around -80 degrees extending on a larger frequency range for PVBA coated steel compared to that corresponds of the SS. The plateau extension in the high frequency area suggests that the alloy is less active in sodium chloride solution, due to PVBA film attached on 304L stainless steel surface.

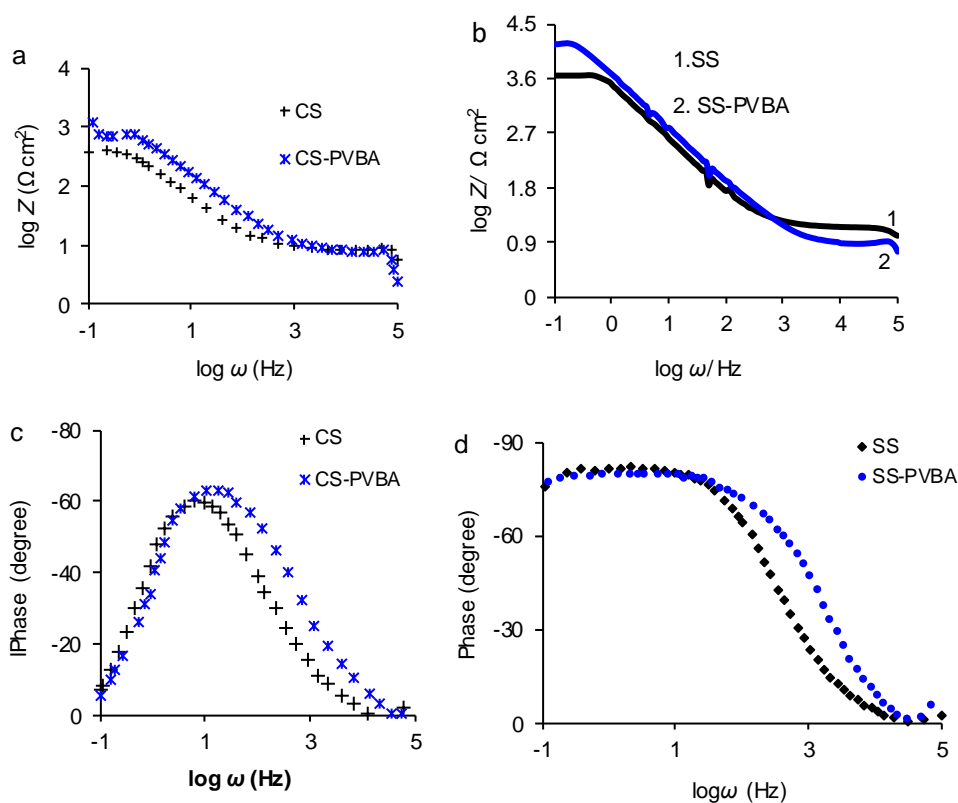


**Figure 3.** Impedance Bode diagrams (a, b) and phase Bode plots (c, d) recorded for uncoated and PVBA coated steels in 0.9% NaCl solution: a, c – carbon steel; b, d – 304L stainless steel

The experimental data were fitted using a three-component equivalent circuit as: the solution resistance ( $R_s$ ) coupled in series with both, charge transfer resistance ( $R_{ct}$ ) linked in parallel with constant phase element (CPE). The electric double-layer capacitance ( $C_{dl}$ ) was replaced with CPE due to some imperfections that appear at metal/electrolyte interface [31]. The correlation index ( $n$ ) between  $C_{dl}$  and CPE is presented in Table 1. As can be observed, the index values are close to unity and consequently, CPE may be assimilated with  $C_{dl}$ , following a capacitive behavior (Table 1) [31]. The performance

protection (P %) of PVBA coating was computed using Equation 1 [24]. All discussed electrochemical parameters and PVBA protection performance were listed in Table 1.

$$P\% = \frac{R_{ct}^{PVBA} - R_{ct}^S}{R_{ct}^{PVBA}} \times 100 \quad (1)$$

where  $R_{ct}^S$  is the charge transfer resistance of uncoated samples and  $R_{ct}^{PVBA}$  represents the charge transfer resistance of PVBA coated samples.

**Table 1.** PVBA protection performance (P %) and electrochemical parameters calculated from electrochemical impedance spectroscopy (EIS) for uncoated (CS and SS) and coated samples (CS-PVBA and SS-PVBA) in 0.9% NaCl solution

Sample	$E_{OCP}$ (mV) vs. AgAgCl	$R_s$ ( $\Omega \text{ cm}^2$ )	$R_{ct}$ ( $\Omega \text{ cm}^2$ )	$C_{dl}$ ( $\mu\text{F cm}^2$ )	n	Log Z ( $\Omega \text{ cm}^2$ )	Z ( $\Omega \text{ cm}^2$ )	Phase (degree)	P (%)
CS	-475	12.1	405	434	0.97	2.7	398	-59.9	-
CS-PVBA	-465	9.7	1075	153	0.99	3.02	1047	-63.1	62.3
SS	-147	17.3	4520	273	0.89	3.66	4571	-81	-
SS-PVBA	-87	10.4	15095	87	0.92	4.18	15135	-79	70.1

Investigating the information from Table 1, it is found that: (1) PVBA coated samples reach higher values of charge transfer resistance ( $R_{ct}$ ) and impedance (Z) than those not-covered, while the electric double-layer capacitance ( $C_{dl}$ ) and the solution resistance ( $R_s$ ) decrease; (2) for the samples of non-coated stainless steel as well as of the one coated with PVBA, higher values of  $R_{ct}$  and Z than those of carbon steel, were obtained; (3) PVBA protection performance (P%) reached a value of 62.3% for carbon steel and 70.1% for stainless steel respectively, indicating a moderate protection efficiency of PVBA film deposited by adsorption from methanol solution using a simple dipping method. Similar results were obtained for PVBA coated copper, when the polymer protection performance determined from EIS reached a value of 80.9% [24].

### 3.3. Potentiodynamic polarization

The potentiodynamic polarization results are shown in Figure 4. In the PVBA film presence, the semilogarithmic polarization curves corresponding to CS-PVBA (Fig. 4a) and SS-PVBA (Fig. 4c) are located in a lower current area than those recorded in the polymeric film absence (CS and SS), indicating that both processes, anodic and cathodic, are restricted due to the blocking of the metal surface active sites by the adsorption of PVBA macromolecules. Thus, the oxidation and reduction processes are attenuated, leading to corrosion current density ( $i_{corr}$ ) decrease and polarization resistance ( $R_p$ ) increase, respectively.

In the presence of PVBA coated samples, more pronounced displacement of the corrosion potential ( $E_{corr}$ ) to higher value is highlighted, in the case of SS-PVBA (Fig. 4c) than that for CS-PVBA sample (Fig. 4a). Moreover, the stainless steel electrochemical behavior is different from that of carbon steel in 0.9% NaCl solution. Carbon steel is active in the anodic domain (Fig. 4a) while for stainless steel

a plateau was recorded, in the potential range between -300 mV and -150 mV, at an approximately constant current density, which is also revealed by the anodic Tafel slopes ( $b_a$ ) that are larger than those of carbon steel (Table 2). On the contrary, the cathodic processes take place with much higher Tafel slopes ( $b_c$ ) for CS than those determined for SS, in the experimental data fitting area, indicating a greater cathodic reaction evolution, in the case of carbon steel. The corrosion current density ( $i_{\text{corr}}$ ) was computed at the intersection of the Tafel lines extrapolated to the corrosion potential ( $E_{\text{corr}}$ ). The polarization resistance ( $R_p$ ) was calculated from the linear diagrams presented in Figs. 4b and 4d obtained by recording the polarization curves in a potential range close to corrosion potential [24, 26-29]. The slopes  $(di/dE)_{E \rightarrow E_{\text{corr}}}$  of the tangents drawn to the polarization curves represent polarization conductance ( $C_p$ ) [24, 26-29].

Practically, deriving the equations inserted in Figs. 4b and 4d,  $C_p$  was obtained and consequently polarization resistance was calculated using Equation 2 [24, 26-29].

$$R_p = 1/C_p \quad (2)$$

As in the case of impedance measurements, the electrochemical parameters namely,  $E_{\text{corr}}$ ,  $i_{\text{corr}}$ ,  $b_a$  &  $b_c$  and  $R_p$  presented in Table 2, were determined using the VoltaMaster software.

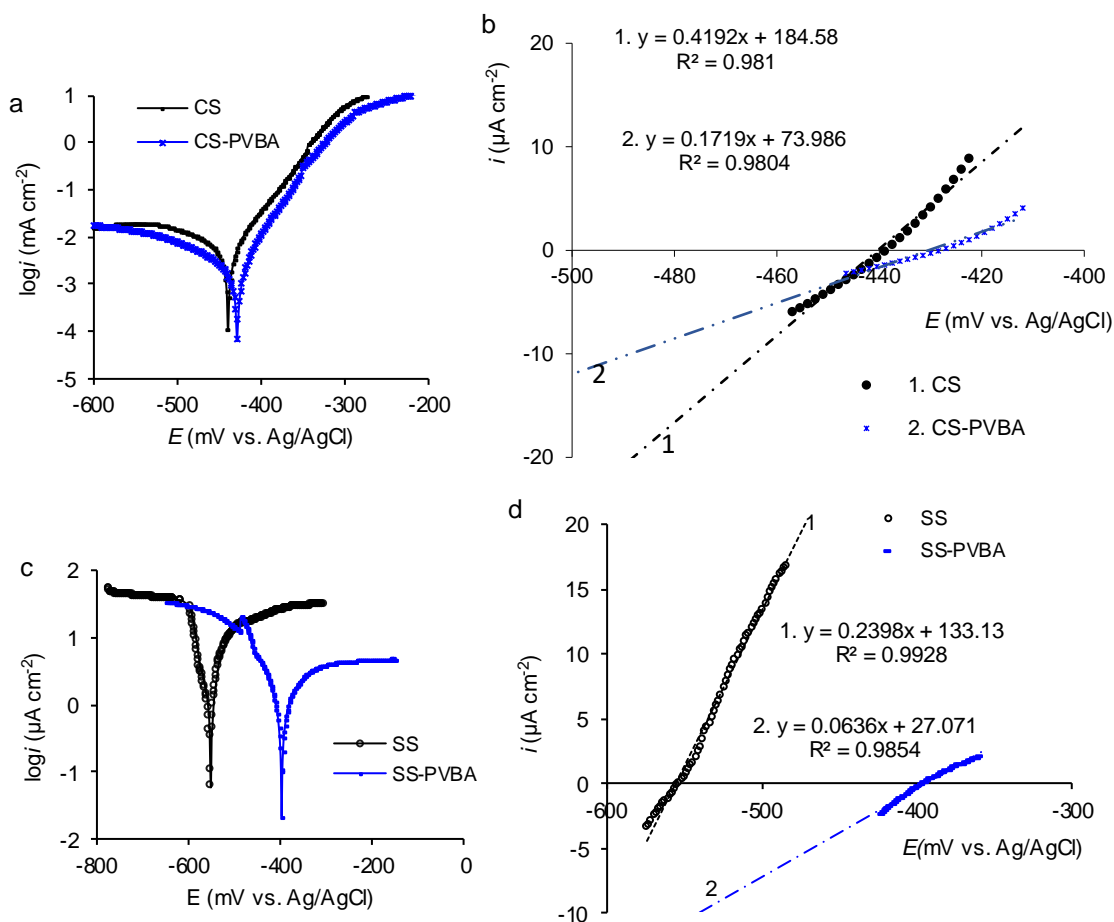


**Figure 4.** Semilogarithmic polarization curves (a, c) and linear diagrams (b, d) recorded for the two types of steel corroded in 0.9% NaCl solution with a potential scan rate of 1.0 mV s<sup>-1</sup>; a, b – carbon steel; c, d – 304L stainless steel.

**Table 2.** PVBA protection performance (P%) and electrochemical parameters obtained from potentiodynamic polarization for uncoated (CS and SS) and coated samples (CS-PVBA and SS-PVBA) in 0.9% NaCl solution

Proba	$E_{\text{corr}}$ (mV) vs. Ag/AgCl	$i_{\text{corr}}$ ( $\mu\text{A cm}^{-2}$ )	$b_a$ ( $\text{mV dec}^{-1}$ )	$ b_c $ ( $\text{mV dec}^{-1}$ )	$C_p 10^3$ ( $\text{S cm}^{-2}$ )	$R_p$ ( $\Omega \text{ cm}^2$ )	P (%)	
							From Tafel	From $R_p$
CS	-439	6.8	45.5	266	0.505	1980	-	-
CS-PVBA	-428	2.3	40.1	133	0.175	5714	66.1	65.3
SS	-553	5.1	135.8	54.8	0.24	4167	-	-
SS-PVBA	-397	1.3	164.8	87.2	0.064	15625	74.5	73.3

PVBA protection performance (P%) was calculated according to  $i_{\text{corr}}$  values obtained from Tafel and using  $R_p$  values deduced from linear diagrams following the Equations 3 and 4, respectively [24, 25].

$$P\% = \frac{i_{\text{corr}}^{\text{S}} - i_{\text{corr}}^{\text{PVBA}}}{i_{\text{corr}}^{\text{S}}} \times 100 \quad (3)$$

$$P\% = \frac{R_p^{\text{PVBA}} - R_p^{\text{S}}}{R_p^{\text{PVBA}}} \times 100 \quad (4)$$

where  $i_{\text{corr}}^{\text{S}}$  and  $R_p^{\text{S}}$  are the corrosion current density and polarization resistance of uncoated steel samples and  $i_{\text{corr}}^{\text{PVBA}}$  and  $R_p^{\text{PVBA}}$  represent the corrosion current density of PVBA coated samples, respectively.

From Table 2, it can be observed that, for the PVBA coated samples (CS-PVBA and SS-PVBA) corroded in 0.9% NaCl solution, the corrosion current density has lower value than that of the uncoated samples (CS and SS), while the polarization resistance has an upward trend.

PVBA protection performance slightly increases than the one was determined from impedance measurements, indicating that the upper surface layer did not deteriorate, after EIS, and PVBA film is stable, still possessing the ability to delay corrosion processes by restricting ion exchange between electrolyte and metal surface.

On the other hand, most likely the slight increase of the protection performance is due to the insertion in the polymeric film of some metal ions (e.g.  $\text{Na}^+$ ,  $\text{Fe}^{2+}$ ,  $\text{Fe}^{3+}$ ) that increase the resistance of the film as well as of the water molecules that favor the swelling of the polymeric film and its extension on a larger surface fraction.

The anticorrosive action of polymer/copolymer coatings was investigated for many metals and alloys in contact with various aggressive environments. Thus, higher PVBA protection performance of 80.1% [24] was computed for copper using potentiodynamic polarization performed in 0.9% NaCl solution, probably due to better adhesion of copolymer film on the substrate, that was favored by the formation of Cu-PVBA complexes which were strongly bound to the metallic surface, and the film desorption was thus delayed.

Another study showed that poly{[(2-methacryloyloxy ethyl) trimethylammonium chloride]-co-N-vinyl-2-pyrrolidone} reached an anticorrosion performance, ranging in function of its concentration between 48% and 87%, for N80 steel tested by potentiodynamic polarization in 3.5% NaCl solution [32].

The copolymer concentration influence as well as the applied method effect were also investigated highlighting that especially, at low concentration of 50-200 ppm a higher performance protection of 76-84% was obtained by EIS, compared to 48-69% calculated from potentiodynamic polarization, while a concentration of 500 ppm leads to a protection efficiency of 87-89% [32].

The anticorrosive action of some copolymers based on polyacrylamide-graft-poly(2-methoxyaniline) [33] and methyl methacrylate/butyl acrylate/acrylic acid [34] was reported for mild steel corroded in 1.0 mol L<sup>-1</sup> HCl solution, revealing for their protection performance, values around 74% [33] and 97% [34], respectively. Also, poly(aniline-co-phenetidine) increases the mild steel corrosion resistance in 3.5% NaCl solution, improving metallic surface anticorrosive properties [35].

The inhibitive effect of polyvinylpyrrolidone on stainless steel corrosion reached a high level of 96.9% for polymer molecular mass of 45000, and contrary a lower value around 43% at molecular mass of 10000 [36]. A good anticorrosion performance for stainless steel was also obtained by modelling the copolymer coatings based on polyvinylpyrrolidone, such as poly{(N-methacryloyloxy methyl) benzotriazole-co-N-vinylpyrrolidone} [37].

### 3.4. Atomic Force Microscopy (AFM)

Figures 5 and 6 show the 3D images acquired by atomic force microscopy (AFM) before (Figs. 5a-c and Figs. 6a-c) and after corrosion (Figs. 5b-d and Figs. 6b-d).

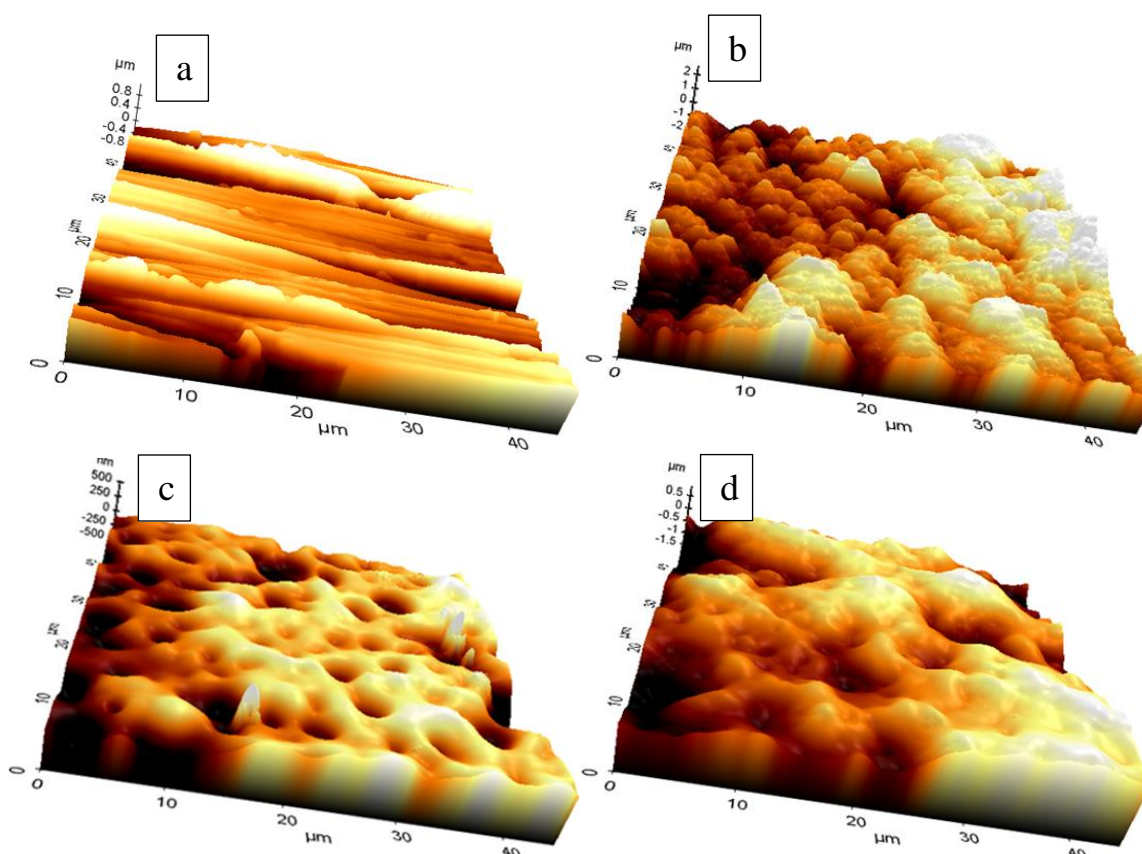


**Figure 5.** AFM 3D images of carbon steel: a – uncoated sample before corrosion; b – after corrosion of bare sample in 0.9% NaCl solution; c – before corrosion of PVBA coated sample; d – after corrosion of PVBA coated sample in 0.9% NaCl solution

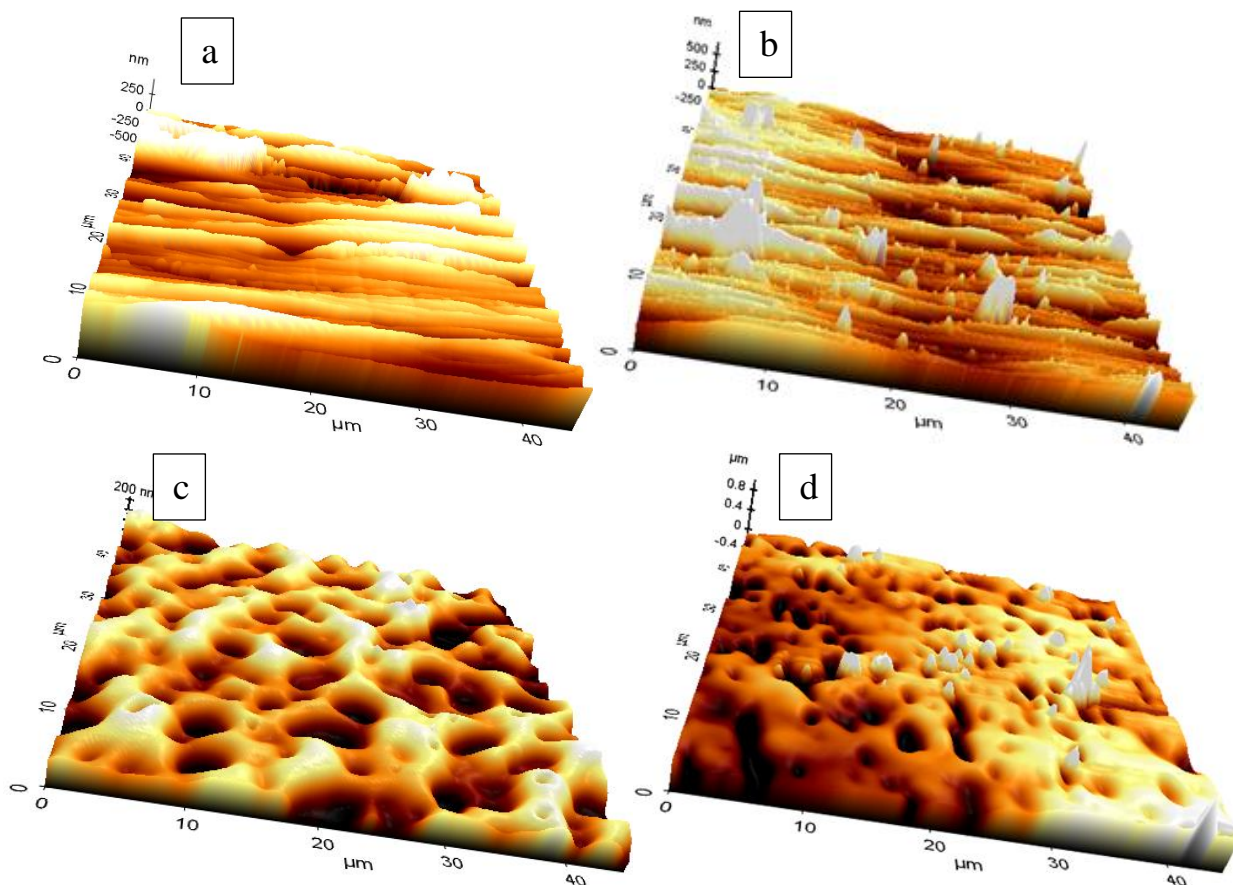


**Figure 6.** AFM 3D images of 304L stainless steel: a – uncoated sample before corrosion; b – after corrosion of bare sample in 0.9% NaCl solution; c – before corrosion of PVBA-coated sample; d – after corrosion of PVBA-coated sample in 0.9% NaCl solution

The steel surfaces are damaged because of corrosion, and the ununiform appearance of coatings can be attributed to the corrosion compounds occurred during potentiodynamic polarization being much better highlighted for carbon steel (Fig. 5b) than for stainless steel (Fig. 6b). Also, the surface layer contains certain inserts of randomly distributed salt deposits, that affect the smoothness and thus emphasizes the coating roughness.

In the case of corroded stainless steel (Fig. 6b), the surface retains some SS characteristics (Fig. 6a), and the surface coverage is completely different from that of carbon steel (Fig. 5b), probably due to the spontaneous passivation of stainless steel in NaCl solution.

Figures 5c and 6c show the distribution of PVBA polymer film on the surface of steels. For both steel types, the coatings display the characteristics of a network, more coherently organized on stainless steel surface (Fig. 6c) than that of carbon steel (Fig. 5c).

After corrosion (Figs. 5d and 6d), the polymer films maintain their appearance, but seem smoother and relatively thicker, probably due to swelling in aqueous NaCl solution during electrochemical measurements. For both steels, no surface areas with similar characteristics to the corroded samples in the film absence are highlighted, suggesting that the PVBA macromolecules were not desorbed from the metallic surfaces. Thus, it is also explained that, after the potentiodynamic polarization, the protection performance slightly increased *versus* that determined from the EIS.

Consequently, the PVBA polymer film is well anchored to the substrates, and the protective performance preservation can be due to its properties of polymer with "shape memory" [24].

The inhibitory effect of the polymeric coatings depends on the metal/alloy nature [24], on the polymer features (e.g. molecular mass, polymerization degree) [36], as well as those of the corrosion environment (e.g. pH, composition) [32], being sometimes influenced, more or less, by the method applied for testing [32]. Thus, by optimizing all the parameters including coating deposition temperature, it is possible to successfully achieve the pretreatment of metal surfaces for different industrial applications.

### 3.5. PVBA action mechanism

The copolymer molecular structure is shown in Figure 7. It is observed that the PVBA presents 3 types of structural units afferent to the polyvinyl butyral (with the greatest polymerization degree), to the polyvinyl alcohol and to the polyvinyl acetate (in a very low percentage). As reported in the literature [23], butyral groups with a hydrophobic character and the -OH groups from the polyvinyl alcohol macromolecule presenting hydrophilic properties favor the binding of PVBA to certain metal substrates such as iron, aluminum tin, lead through noncovalent interactions (hydrogen bonds) or metallic coordination [39, 40] creating a host-guest interaction between metal matrix and copolymer, respectively.

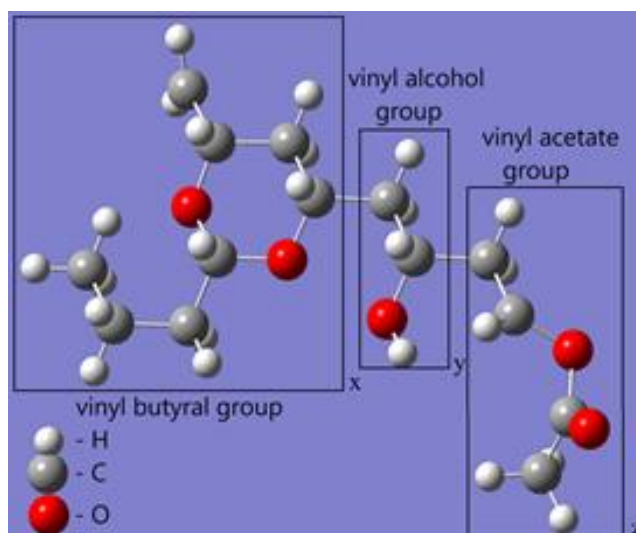


**Figure 7.** Molecular structure of poly(vinyl butyral-co-vinyl alcohol-co-vinyl acetate);  $x:y:z = 39:29:1$

For both steels there are competitive adsorption processes of methanol molecules and PVBA macromolecules. Most likely, the methanol molecules are primarily adsorbed on the steel surface because of the macromolecular chain steric arrangement can prevent its diffusion at the metal/electrolyte interface. Thus, the hydrogen-bridged can form between adsorbed methanolic hydroxyl groups and those of the polyvinyl alcohol fraction from PVBA macromolecule.

At the same time, the coordinative bonds are formed between the free electron pairs of the oxygen atoms belonging to the butyral and acetate groups and the vacant “*d*” orbital of the iron atoms, which ensures a moderate chemical adsorption of the PVBA macromolecules. Thus, a synergistic mechanism can be assumed between physical adsorption through hydroxyl groups and chemical adsorption primarily through the butyral groups, the acetate groups participating to a lesser extent.

Due to the hydrophilic groups, when the samples are immersed in NaCl solution, the increase of the swelling capacity of upper-surface layer takes place followed by the polymeric film thickness increase and its extension development on the metallic surface.

This can favor a superficial detachment of the coating on the metal surface more pronounced in the case of carbon steel than the one of stainless steel, which also explains the lower protection performance for carbon steel than that for stainless steel.

Based on experimental date, it can conclude that for both steels, the hydroxyl groups favor the insertion of water/sodium chloride molecules in the copolymer matrix in a greater manner than in the case of copper, when  $\text{Cu}^+$  and  $\text{Cu}^{2+}$  ions promote the crosslinking reaction of polyvinyl alcohol from PVBA macromolecules [38] and consequently, the occurrence of copolymer complexes [24], that provide a better adhesion and copper surface protection.

#### 4. CONCLUSIONS

Poly(vinyl butyral-co-vinyl alcohol-co-vinyl acetate) referred to as PVBA film was obtained by pure adsorption from methanolic solution using the simple dipping method.

A synergic action mechanism between physical absorption of polyvinyl alcohol fraction and chemical adsorption of polyvinyl butyral and polyvinyl acetate macromolecular chains, can be approached to explain the PVBA film attachment on the surface of the two steels.

After consecutive electrochemical measurements performed on bare steel electrodes and PVBA coated samples, it was found that the copolymer provides a protection performance of approximately 66% for carbon steel and 74% for stainless steel.

Due to the fact that the protection performance increases, after potentiodynamic polarization compared to that obtained from EIS, it is estimated that the polymer can withstand a relatively long time on the metal surface because the coating anticorrosive resistance reaches a high level due to ionic insertions, that change the surface chemistry and improve upper-surface layer adhesion.

#### References

1. K. Alaoui, Y. El Kacimi, M. Galai, R. Tourir, K. Dahmani, A. Harfi and M. Ebn Touhami, *J. Mater. Environ. Sci.*, 7 (2016) 2389.
2. A. Samide, B. Tutunaru, C. Merisanu and N. Cioatera, *J. Therm. Anal. Calorim.*, 2020 <https://doi.org/10.1007/s10973-020-09489-y>.
3. A. Biswas, D. Das, H. Lgaz, S. Pal and U. G. Nair, *J. Mol. Liq.*, 275 (2019) 867.
4. S. C. Nwanonyi, O. Ogbobe, I. C. Madufor and E. E. Oguzie, *Eur. J. Adv. Eng. Tech.*, 3 (2016) 52.
5. A. Samide, C. Stoean and R. Stoean, *Appl. Surf. Sci.*, 475 (2019) 1.

6. O. Sanni, O. S. I. Fayomi and A. P. I. Popoola, *J. Phys. Conf. Ser.*, 1378 (2019) 042047, doi:10.1088/1742-6596/1378/4/042047.
7. S. Kaviyarasu, S. Anandakumar, K. Vignesh and G. S. Rampradheep, *Int. J. Sci. Techn. Res. (IJSTR)*, 9 (2020) 2888.
8. A. Samide, C. Negrila and A. Ciuciu, *Dig. J. Nanomater. Bios.*, 5 (2010) 1001.
9. S. A. Umoren, M. J. Banera, T. Alonso-Garcia, C. A. Gervasi and M. V. Mirífico, *Cellulose*, 20 (2013) 2529.
10. A. Yabuki, S. Tanabe and I. W. Fathona, *Surf. Coat. Tech.*, 341 (2018) 71.
11. R. Jeyaram, A. Elango, T. Siva, A. Ayeshamariam and K. Kaviyarasu, *Surf. Interface*, 18 (2020) 100423 <https://doi.org/10.1016/j.surfin.2019.100423>.
12. A. Singh, N. Soni, Y. Deyuan and A. Kumar, *Results Phys.*, 13 (2019) 102116.
13. S. Jadoun and U. Riaz, *Polym.-Plast. Technol. Mat.*, 59 (2020) 484.
14. X. Li, S. Deng, T. Lin, X. Xie and G. Du, *J. Mater. Res. Technol.*, 9, (2020) 2196.
15. S. Xue, Y. Ma, Y. Miao and W. Li, *Int. J. Nanosci.*, (2020) 1950023.
16. H. Wang, P. Zhang, G. Fei, Y. Ma, N. Rang and Y. Kang, *Prog. Org. Coat.*, 137 (2019) 105274.
17. H. M. A. El-Salam, G. M. A. El-Hafez, H. G. Askalany and A. M. Fekry, *J. Bio. Tribo-Corros.*, 6 (2020) 53.
18. G. Achary, Y. A. Naik, S. V. Kumar, T. V. Venkatesha and B. S. Sherigara, *Appl. Surf. Sci.*, 254 (2008) 5569.
19. A. Madhankumar and N. Rajendran, *Synth. Met.*, 162 (2012) 176.
20. D. Gopi, P. Karthikeyan, L. Kavitha and M. Surendiran, *Appl. Surf. Sci.*, 357 (2015) 122.
21. Y. Lin, A. Singh, E. E. Ebenso, Y. Wu, C. Zhu and M. Zhu, *J. Taiwan Inst. Chem. E.*, 46 (2015) 214.
22. Y. Bai, Y. Chen, Q. Wang and T. Wang, *J. Mater. Chem. A.*, 2 (2014) 9169.
23. P. Kumar, N. Khan and D. Kumar, *Green Chem. Tech. Letters*, 2 (2016) 185.
24. A. Samide, C. Merisanu, B. Tutunaru and G. E. Iacobescu, *Molecules*, 25 (2020) 439. <https://doi.org/10.3390/molecules25030439>.
25. A. Samide, G. Bratulescu, C. Merisanu and N. Cioatera, *J. Appl. Polym. Sci.*, 136 (2019) 47320. <https://doi.org/10.1002/app.47320>.
26. A. Samide, G. E. Iacobescu, B. Tutunaru, R. Grecu, C. Tigae and C. Spînu, *Coatings*, 7 (2017) 181; <https://doi.org/10.3390/coatings7110181>.
27. A. Samide, G. E. Iacobescu, B. Tutunaru and C. Tigae, *Int. J. Electrochem. Sci.*, 12 (2017) 2088.
28. A. Samide, S. Iordache, G. E. Iacobescu, C. Tigae, C. Spînu, *Int. J. Electrochem. Sci.*, 13 (2018) 12125.
29. A. Samide, R. Grecu, B. Tutunaru, C. Tigae and C. Spînu, *Int. J. Electrochem. Sci.*, 12 (2017) 11316.
30. A. Samide, P. Ilea and A. C. Vladu, *Int. J. Electrochem. Sci.*, 12 (2017) 5964.
31. A. Samide and B. Tutunaru, *J. Therm. Anal. Calorim.*, 127 (2017) 863.
32. A. Singh, Y. Caihong, Y. Yaocheng, N. Soni, Y. Wu and Y. Lin, *ACS Omega*, 4 (2019) 3420.
33. E. M. S. Azzam, H. M. A. El-Salam, R. A. Mohamed, S. M. Shaban and A. Shokry, *Egypt. J. Pet.* 27 (2018) 897.
34. M. V. Azghandi, A. Davoodi, G. A. Farzi and A. Kosari, *Metallurg. Mater. Trans. A*, 44A (2013) 5493.
35. P. Sambyal, G. Ruhi, R. Dhawan and S. K. Dhawan, *Surf. Coat. Tech.*, 303 (2016) 362.
36. M. M. Khaled, *Arab. J. Sci. Eng.*, 35 (2010) 29.
37. K. M. Govindaraju, D. Gopi and K. A. Basha, *J. Appl. Electrochem.*, 43 (2013) 1043.
38. J. Gong, L. Luo, S.-H. Yu, H. Qian and L. Fei, *J. Mater. Chem.*, 16 (2006) 101.
39. Z. C. Jiang, Y. Y. Xiao, Y. Kang, M. Pan, B. J. Li and S. Zhang, *ACS Appl. Mater. Interfaces*, 9 (2017) 20276.

40. C. Carrot, A. Bendaoud, C. Pillon, *Chapter 3. Polyvinyl Butyral*, in book: Handbook of Thermoplastics, CRC Press, 22 Dec 2015, pp. 128.

© 2020 The Authors. Published by ESG ([www.electrochemsci.org](http://www.electrochemsci.org)). This article is an open access article distributed under the terms and conditions of the Creative Commons Attribution license (<http://creativecommons.org/licenses/by/4.0/>).